Hum Genet (2002) 110 : 157–165
DOI 10.1007/s00439-001-0655-5

ORIGINAL INVESTIGATION

**Patric Schön · Ken Tsuchiya · Didier Lenoir · Toshio Mochizuki · Cécile Guichard · Setsuo Takai
Amit K. Maiti · Hiroshi Nihei · Johan Weil · Takahiko Yokoyama · Patrice Bouvagnet**

Identification, genomic organization, chromosomal mapping and mutation analysis of the human *INV* gene, the ortholog of a murine gene implicated in left-right axis development and biliary atresia

Received: 21 August 2001 / Accepted: 31 October 2001 / Published online: 18 December 2001

Abstract Determination of left-right axis is a precocious embryonic event, and all phenotypic anomalies resulting from disruption of the normal lateralization process are collectively referred to as the lateralization defect. A transgenic mouse with lateralization defect and hepatic, kidney, and pancreatic anomalies has resulted from disruption of the *inv* gene by insertion of a transgene. The human ortholog is thus a good candidate for lateralization defect in humans, in particular in cases with associated hepatic anomalies. Here, we have identified, mapped, and characterized the *INV* human gene and screened a series of heterotaxic patients (with or without biliary anomalies) for mutation in this gene. In a German family of Turkish origin, we have found that all available affected and unaffected individuals are heterozygous for a mutation in the splicing donor site of intron 12 in the *INV* gene resulting in two different aberrant splicing isoforms. This can be explained either by a randomization of lateralization defects or, as suggested earlier, di- or trigenic inheritance, although we have been unable to detect, in this family, a mutation in genes known to be involved in the human lateralization defect (*LEFTY1*, *LEFTY2*, *ACVR2B*, *NODAL*, *ZIC3*, and *CFC1*). In contrast to the mouse, the affected individuals have no biliary anomalies, and the absence of mutation in a series of seven cases with lateralization defect and biliary anomalies demonstrates that *INV* is not frequently involved in such a phenotype in humans.

Electronic-database information: accession numbers and URLs for the data in this article are as follows:
BLAST Sequence Similarity Search, http://www.ncbi.nlm.nih.gov/BLAST/
Centre de Ressources INFOBIOGEN, http://www.infobiogen.fr/srs/ (accession nos. AF039217, AF034860; NT_008513)
Online Mendelian Inheritance in Man (OMIM), http://www.ncbi.nlm.nih.gov/Omim
PROSITE, Database of Protein Families and Domains, http://www.expasy.ch/prosite

P. Schön · D. Lenoir · C. Guichard · A.K. Maiti
P. Bouvagnet (✉)
Laboratoire de Génétique Moléculaire Humaine,
EA 3088, Faculté de Médecine Pharmacie,
Université C. Bernard Lyon 1,
8 Avenue Rockefeller, 69373 Lyon cedex 8, France
e-mail: pbouv@rockefeller.univ-lyon1.fr,
Tel.: +33-478-777121, Fax: +33-478-777568

P. Bouvagnet
Service de Cardiologie Pédiatrique, Hôpital Cardiologique,
Lyon, France

P. Schön
Kinderklinik, Deutsches Herzzentrum München,
Technische Universität München, München, Germany

J. Weil
Abteilung für Kinderkardiologie,
Universität Krankenhaus Eppendorf, Hamburg, Germany

K. Tsuchiya · T. Mochizuki · H. Nihei
Fourth Department of Internal Medicine,
Tokyo Women's Medical College, Tokyo, Japan

T. Yokoyama
Department of Anatomy and Developmental Biology,
Tokyo Women's Medical College, Tokyo, Japan

S. Takai
Department of Genetics, Research Institute,
International Medical Center of Japan, Tokyo, Japan

Introduction

During embryonic development in vertebrates, the earliest organ lateralization process is the looping of the heart tube on the right side. This phenomenon represents only part of the lateralization that corresponds to the asymmetric positioning of all internal organs along the left-right axis. For example, the major lobe of the liver lies on the right side of the abdomen, whereas the spleen and the stomach are on the left side. About one person in 10,000 is born with anomalies of the left-right axis determination. For partial (situs ambiguus) or complete (situs inversus) reversion of visceral organ position, we will hereafter refer to any abnormal positioning of an organ as the lateralization defect. The lateralization defect is often associated with cardiovascular malformations, ciliary dyskinesia (referred to as Kartagener syndrome), hepatic, renal, or mid-

line anomalies. The transmission mode of the lateralization defect is heterogeneous. Exceptionally, it is X-linked recessive (Mathias et al. 1987) or semi-dominant (Mikkilä et al. 1994; Gebbia et al. 1997), and the gene *ZIC3* is involved in several of these families (Gebbia et al. 1997). Surprisingly, non-penetrance in a male carrying a mutation in *ZIC3* has been demonstrated for the first time in X-linked inheritance (Mégarbané et al. 2000). This gene codes for a peptide with five putative zinc finger domains, and mutation in *ZIC3* are often associated with the transposition of the great arteries (Gebbia et al. 1997; Mégarbané et al. 2000), suggesting that it might be the genetic factor for this cardiac malformation, which affects twice as many boys as girls. In rare families, inheritance of the lateralization defect is autosomal dominant (Chen and Monteleone 1977; Niikawa et al. 1983; Alonso et al. 1995; Lindor et al. 1995; Casey et al. 1996; de Meeus et al. 1997). So far, the most common inheritance mode of the lateralization defect is thought to be autosomal recessive (Bowers et al. 1996), although this has never been demonstrated at the molecular level, despite considerable effort in screening for mutation in several genes with asymmetric expression during embryonic development: *ZIC3* (Gebbia et al. 1997), *NODAL* (Gebbia et al. 1997), *LEFTY1* (Kosaki et al. 1999a), *LEFTY2* (Kosaki et al. 1999a), *ACVR2B* (Kosaki et al. 1999b), and *CFC1* (Bamford et al. 2000). Only heterozygotes or, exceptionally, double heterozygotes have been found suggesting that autosomal recessive inheritance might be rare compared with double (or triple) heterozygotes (Casey 1998).

For a better understanding of the molecular mechanisms involved in the determination of left-right axis, animal models are important. Several mouse lines are affected by lateralization defects, in particular, *iv* (inversus viscerum) and *inv* (inversion of the embryonic turning). The transmission mode is autosomal recessive, and penetrance varies depending on the mutation. The mutated genes are, respectively, the *lrd* gene (*left right dynein*), encoding a dynein heavy chain and mapping to murine chromosome 12 (Supp et al. 1997), and the *inv* gene mapping to murine chromosome 4 (Mochizuki et al. 1998). Mice homozygous for the *inv* mutation have lateralization defects, heart malformations, dilated tubules of kidneys, and anomalies of the biliary tract resulting in severe jaundice (Yokoyama et al. 1993). Although the precise role of the inv protein is not yet known, it is a good candidate for the lateralization defect in humans. In this report, we present the identification of the *INV* gene in human, its genomic organization, tissue expression, chromosomal mapping, and mutation screening in patients with various anomalies, including lateralization defects, heart malformations, and biliary tract anomalies. Only an affected brother and sister were found to be heterozygous for a splicing site mutation, although this mutation was also found in two normal siblings and both consanguineous parents.

Materials and methods

mRNA experimentations

A human fetal brain cDNA library (Clonetech) was screened with full length mouse *inv* cDNA. A positive clone (H2C) was obtained and sequenced. The human fetal brain and a human kidney cDNA libraries were then screened with human clone H2C. Two additional clones were obtained (714.2b and HK904-8). To obtain the 5' and 3' ends of human *INV* cDNA, rapid amplification of cDNA ends (RACE) was performed with the kidney cDNA library and the Life Technologies kit.

The updated human *INV* cDNA sequence identified in this study is available in databases under accession no. AF039217. Multiple-tissue human fetal and adult Northern blots (Clontech) were hybridized with the 2.0-kb fragment from pH2C, which was labeled by random priming (Primeit II kit, Stratagene) with 32P-dCTP. Membranes were hybridized with a probe in express hybridization buffer (Clontech) at 60°C overnight, washed in 0.5×SSC (1×SSC=150 mM NaCl, 15 mM sodium citrate, pH 7.0) at 60°C, and then exposed.

Human bacterial-artificial-chromosome genomic clones

Bacterial artificial chromosome (BAC) clones were obtained from Genome systems (St. Louis, Mo.). Clones H2C and HE904-8 were used as probes. BAC clones 211(K10) and 257(H3) were positive for probe H2C, and BAC clones 179(B22), 176(O3), and 211(K10) were positive for probe HK904-8. The genomic structure of the gene was determined by (1) building a restriction map of the BAC clones, (2) cloning and partial sequencing of fragments containing coding sequences, and (3) taking into account the structure of the mouse *inv* gene. Later, these data were confirmed by comparing the cDNA sequence of *INV* with the human genomic sequence obtained by a homology search with BLAST in a genomic databank (Centre de Ressources INFOBIOGEN, http://www.infobiogen.fr/srs/). Exon positions were derived by a comparison between the cDNA and genomic sequences with the software *cross_match* (P. Green, University of Washington).

Mapping of the human *INV* gene by fluorescence in situ hybridization

R-band human chromosomes were prepared from lymphocytes of a healthy male (Viegas-Pequignot and Dutrillaux 1978; Takahashi et al. 1990). Human BAC clones were labeled by nick-translation with biotin-16-dUTP (Roche) as reported previously (Takahashi et al. 1991) and used as a probe for fluorescence in situ hybridization (FISH). Background signals were reduced by competition with human genomic sequences added to the hybridization solution. Standard FISH methods (Lawrence et al. 1988) were performed with some modifications (Takahashi et al. 1991) including a final staining with propidium iodide. The slides were observed by using a Nikon OPTIPHOT-2-EFD2 microscope (B-2A filter for R-bands, UV-2A filter for G-like-bands) and photographed on Fuji chrome film (Sensia, ASA100).

Mutation screening

Blood samples were obtained after informed consent. To search for mutations in *INV*, 15 of the 16 coding exons of the gene were amplified by the polymerase chain reaction (PCR) with a single pair of intronic primers (Table 1). Exon 14 (the longest) required four pairs of overlapping primers (HINV14-1F/R to HINV14-4F/R). Amplified fragments were electrophoresed by single-strand conformation polymorphism (SSCP) at 7°C and 20°C on a 10% acrylamide gel (acrylamide/bisacrylamide: 29/1) with 1×TBE buffer (0.09 M TRIS-borate, 0.002 M EDTA, pH 8.3) at 16 mA per gel, for 2 h 30 min to 6 h (depending on the size of each fragment).

Table 1 PCR primers for SSCP analysis of human *INV* gene

Forward primer	Sequence	Reverse primer	Sequence	Product size (bp)
HINV2F	TGCTAAGAAGACTATGAAC	HINV2R	AACTTCCTCAGGACAAAC	177
HINV3F	TATCACTATCTGTTTCTTATCC	HINV3R	ACATCACACAAAACATTTACTC	240
HINV4F	GACCCCATAGTACATTTTTTTC	HINV4R	TTAGTCTTTGATTTTGAGTATCC	250
HINV5F	TATGTCTGAAGTCTCTGGTTCC	HINV5R	GTTCCTTTTACTGTTGATCCTTTG	247
HINV6F	TATGTCTGAAGTCTCTGGTTCC	HINV6R	GTTCCTTTTACTGTTGATCCTTTG	247
HINV7F	TTACCTTTTTGTGTCTTTTCTC	HINV7R	AGCATTGTCTTGTTTTACTTAC	156
HINV8F	GAAAATACTACTGTTTTGTCTCC	HINV8R	ATGAAAGCAAATTGAATGTGTCC	256
HINV9F	GTTCATCACTTTCTGTTGG	HINV9R	TGTACTTGTGCAGCTTTC	291
HINV10F	CTCCTACTCATTTTAATAAAAGC	HINV10R	AGCAAACAATATAGAAAAGACAG	321
HINV11F	ACTTACTCCAGATGTACTTG	HINV11R	AGCCATCTCAAAAAAAAAAAAAAAAGTC	188
HINV12F	AAAAGAATCTTCCTCCCAC	HINV12R	TGGCGAAAACGCAATCTG	271
HINV13F	CTTCTTTGGCTTTGCTTC	HINV13R	GATGACAAAGGCAATACAC	328
HINV14-1F	GGAAAATTATCCTACTCTGCAAG	HINV14-1R	CTTCCAGTGGCTATCGTG	313
HINV14-2F	TGATGAGAAAGGAGAGGACTCCAG	HINV14-2R	GTGCTCTGTGGCAAATGTGAATAG	297
HINV14-3F	AAT CCT CCC CAC CAT CGT ACAC	HINV14-3R	GATGACTGCTGCTGCCTTGTTC	299
HINV14-4F	CCTGTCCGAGGACTTTCAGGTATC	HINV14-4R	CAGTAACAAAGAACCACAGATGCG	233
HINV15F	ATCTTAAAGCCTCTCCTC	HINV15R	GAACTACAAAGTAGGCAG	309
HINV16F	AAAGCCTCTCCTCTCCTCTG	HINV16R	CATGAGACCCCCATGAACAC	238
HINV17F	TCAACACCAATGAACTATTCCC	HINV17R	GATTATCAGCAGAAAATCTGAAC	256

When bandshifts were identified, the corresponding PCR products were sequenced in both directions.

The splicing defect was tested on lymphocyte RNA extracted with Promega's kit (reagent total RNA isolation system). Reverse-transcription/PCR (RT-PCR) was carried out with SuperScript II RNAse H-reverse transcriptase (Life Technologies) and primer 5'-AGC AGA AAG GAA ACA TTC TGA C-3', which hybridizes in the 3'-untranslated region (3'-UTR), to obtain the first cDNA strand, and primers 5'-ACA AGG TCA GAA AAG CCT TC-3' (sense) and 5'-GAT CTC TCC TTT CTC ATC AG-3' (antisense), which hybridize to exons 12 and 14, respectively, to amplify the fragment (hybridization temperature: 54°C). PCR products were run on a 1.3% agarose gel. The two small aberrant bands were gel-purified and cloned in a pGEM-T vector system (Promega); at least five clones were sequenced.

LEFTY1, *LEFTY2*, *NODAL*, *ACVR2B*, *ZIC3*, and *CFC1* were amplified by PCR from genomic DNA (primer sequence available upon request), and mutation screening was performed by SSCP and eventually PCR sequencing when band shifts were evidenced.

Results

Identification and characterization of the human *INV* gene

By screening human kidney and fetal cDNA libraries with a probe of mouse *inv* cDNA, three clones were recovered that overlapped: 714.2b, HK904-8, and H2C (Fig. 1A). To obtain the 3' and 5' ends of the cDNA, extension was carried out by RACE. Two additional clones were obtained at the 3' and 5' ends: HK8, HK9, and HR13, HR14, respectively. The entire open reading frame with the 3'-UTR and some 5'-UTR were sequenced. The first exon is non-coding. The *INV* cDNA contains a 3195-bp open reading frame coding for 1065 amino acids (Fig. 1B). The gene is composed of 17 exons, of which 16 are coding exons (Fig. 1C). All donor and acceptor sites are GT and AG, respectively. The gene covers about 100 kb with several introns of 10 kb or more.

A stretch of 16 ankyrin repeats was noted at the N-terminal part of the open reading frame starting at residue 13 (schematically represented in Fig. 1B). The carboxy-terminal half of the peptide contains two transcriptional factor interaction sites, named IQ, and a pair of nuclear localization signal-bipartite (NLS-BP; Fig. 1B). The ankyrin repeat is composed of about 33 residues some of which are highly conserved, whereas others are variable. These 16 repeats are aligned beneath the consensus ankyrin repeat in Fig. 2 (PROSITE, Database of Protein Families and Domains, http://www.expasy.ch/prosite). The conservation of residue sequence is extremely high between mouse and human in the ankyrin region over a stretch of 545 amino acids (similarity 100%, identity 97.7%; Fig. 3). This homology confirms that we had selected the methionine corresponding to the correct initiation of translation (Mochizuki et al. 1998). The high homology extends to the first IQ and NLS domains (100% homology). The carboxyl-terminal end of the peptide is much less conserved, although some short stretches of identities suggest domains of unknown functions.

INV is expressed at low level in a wide range of tissues as can be seen on Northern blots (Fig. 4). Besides a band of about 4.2 kb, some tissues present a shorter band of about 3.5 kb. This band, which might correspond to a splicing isoform, is the strongest in liver.

Chromosomal mapping of the human *INV* gene

Among 25 human (pro)metaphase cells hybridized with the probe and microscopically observed, all cells revealed

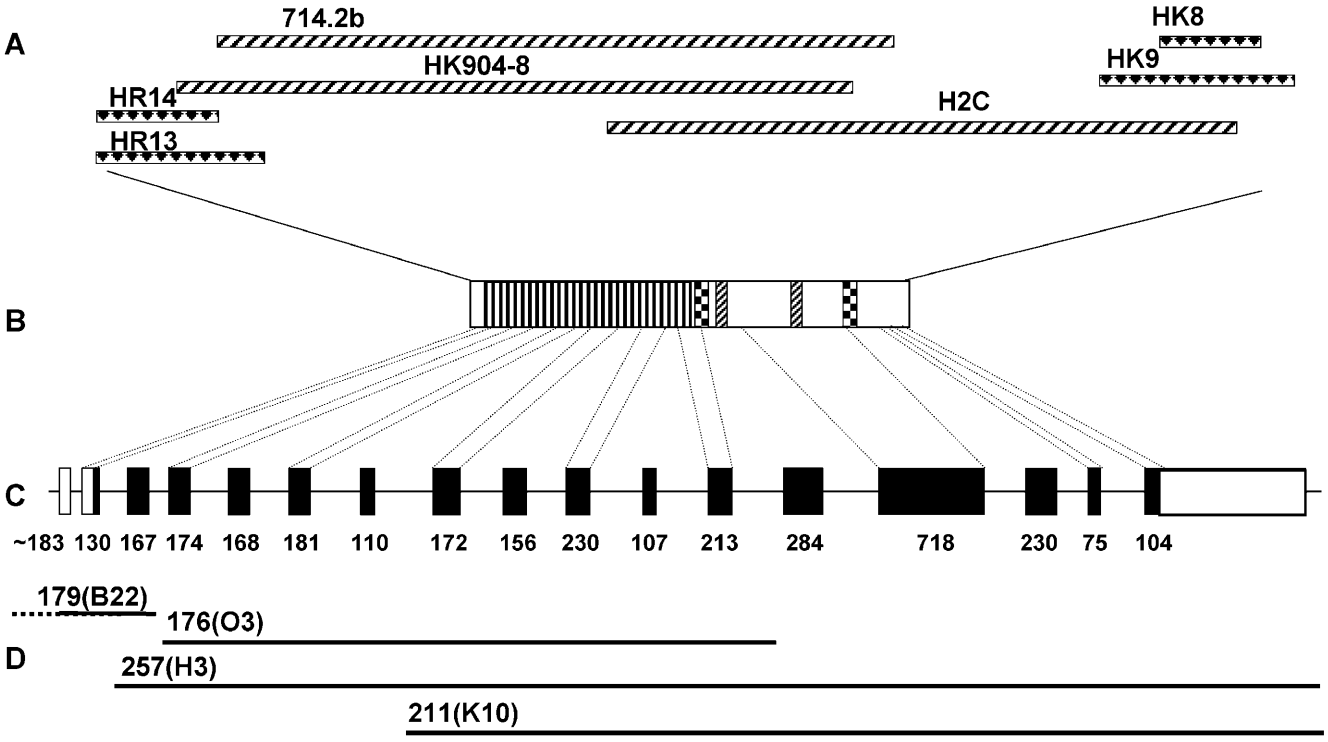

Fig. 1A–D Schematic presentation of human *INV* gene. **A** cDNA clones obtained by screening human kidney and fetal libraries with the *inv* mouse probe and extension of initial clones with RACE. **B** Domains encoded by *INV*: *rectangle with vertical stripes* ankyrin domains, *rectangles with checks* IQ domains, *oblique stripes* nuclear localization signal-bipartite domains. **C** Genomic structure of the human *INV* gene. *Numbers* Exon size in nucleotides, *open rectangles* non-coding regions, *filled rectangles* coding regions. The 17 exons are represented (including the first non-coding exon) with the intronic sequence approximately to scale. **D** BAC clones

symmetrical double spots on both chromosomes 9 at band q22.3-q31.1 (Fig. 5). No other prominent spots were observed. Thus, we conclude that the human gene encoding *INV* is located on human chromosomal region 9q22.3-q31.1. This FISH mapping is in agreement with the human genomic sequence, since the contig NT_008513, which contains the *INV* gene, is located in 9q31. This is also consistent with *inv* mapping to the mouse syntenic region of chromosome 4.

Mutation screening in heterotaxic patients

We screened 65 patients with the lateralization defect (situs inversus totalis or situs ambiguus) for mutation in the human *INV* gene. In this series, 19 individuals were born to consanguineous parents, and 19 were familial cases. In addition to the lateralization defect, 44 had various types

Fig. 2 Alignment of the 16 ankyrin repeats of *INV*. *Top* Ankyrin repeat consensus; *bold* conserved residues, *X* non-conserved residues, *arrowheads* and *rectangles* β-hairpins and α-helices that are characteristic of the ankyrin repeat architecture, respectively. The 16 ankyrin repeats of *INV* are aligned *underneath* with conserved residues in *bold*. *Right* Position of the last residue in each of the tandem repeats

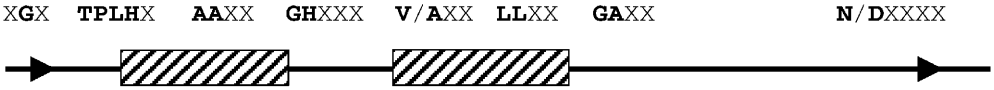

SLA	SQV**H**A	**AA**VN	**G**DKG	**A**LQR	**L**IV	**G**NSALKDKE	**D**Q	46
F**G**R	**TPL**MY	CVL	ADRLDC	**A**DA	**LL**KA	**GA**DVNKT	**D**H	79
SQR	**TALHL**	**AA**QK	**G**NYRF	MKL	**LL**TR	R**A**NWMQK	**D**L	112
EEM	**TPLH**L	TTRH	RSPKC	LAL	**LL**KF	M**A**PGEVDTQ	**D**K	147
NKQ	**TALH**W	S**A**YY	NNPEH	**V**KL	**L**IKH	DSNIGIP	**D**V	180
E**G**K	I**PLH**W	**AA**NH	KDPSA	**V**HT	VRCI	LDAAPTESLLNWQ	**D**Y	219
E**G**R	**TPLH**F	**A**VAD	**G**NVTV	**V**DV	**L**TSY	ESCNITSY	**D**N	253
LFR	**TPLH**W	**AA**LL	**GH**AQI	**V**HL	**LL**ER	NKSGTIPS	**D**S	287
Q**G**A	**TPLH**Y	**AA**QS	NFAET	**V**KVF	**L**KH	PSVKDDS	**D**L	320
E**G**R	**T**SFMW	**AA**GK	**G**SDD	**V**LRTM	**L**SL	KSDIDINMA	**D**K	355
Y**G**G	**TALH**A	**AA**LS	**GH**VST	**V**KL	**LL**EN	N**A**QVDAT	**D**V	388
MKH	**TPL**FR	**A**CEM	**GH**KD	**V**IQT	**L**IKG	**GA**RVDLV	**D**Q	421
D**G**H	SL**LH**W	**AA**LG	**G**NAD	**V**CQI	**L**IEN	KINPNVQ	**D**Y	454
A**G**R	**TPL**QC	**AA**YG	**G**YINC	MAV	**L**MEN	N**A**DPNIQ	**D**K	487
E**G**R	**TALH**W	SCNN	**G**YLDA	IKL	**LL**DF	A**AF**PNQMEN	NE	522
ERY	**TPL**DY	**A**LL	**G**ERHE	**V**IQF	M**L**EH	**GA**LSIAAIQ	**D**I	557

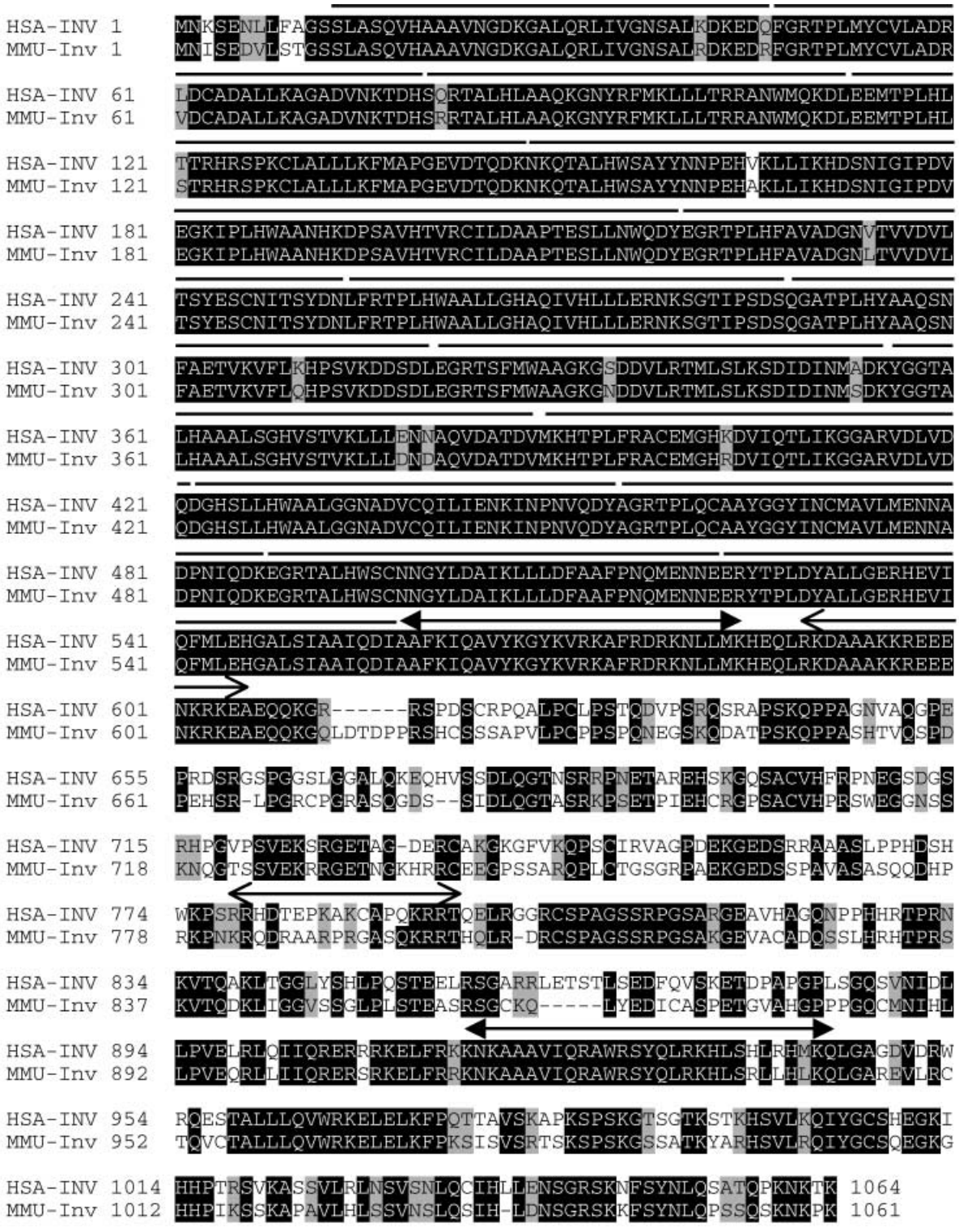

Fig. 3 Comparison of deduced amino acid sequences of human *INV* and mouse *inv*. Identical residues are denoted by a *black background*, similar residues are *shaded*. The 16 ankyrin tandem repeats are marked by *horizontal bars*. IQ domains are marked with a *horizontal bar* beginning and ending with a *filled arrowhead*, whereas NLS-BP domains have *open arrowheads*. Gaps introduced to optimized the alignment are denoted by *dashes* (BLAST Sequence Similarity Search). Note the very high conservation in the first half of the peptides including the whole ankyrin region

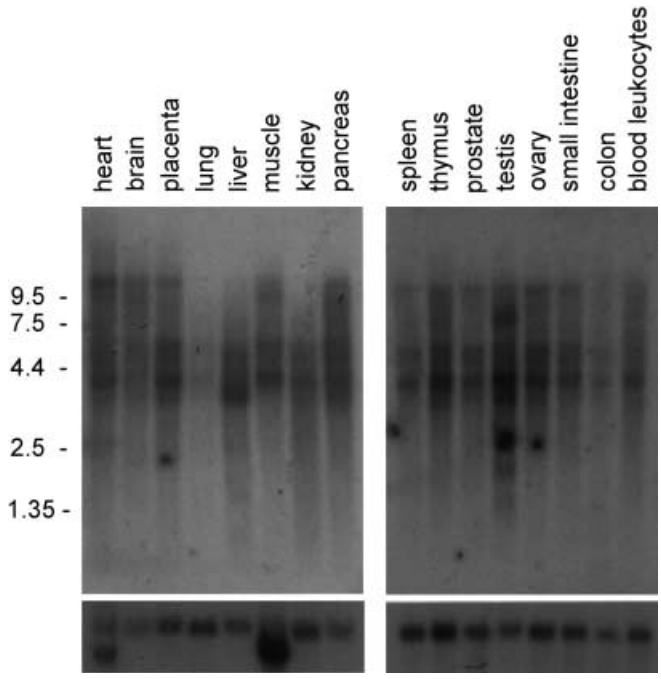

Fig. 4 Northern blot of adult tissues hybridized with the INV cDNA probe. A faint band at about 4 kb is evident in most tissues. Note that liver has a shorter band suggesting a splicing isoform. As a control, the same blot was hybridized with a β-actin probe (*below*). The positions of bands of known sizes are indicated *left*

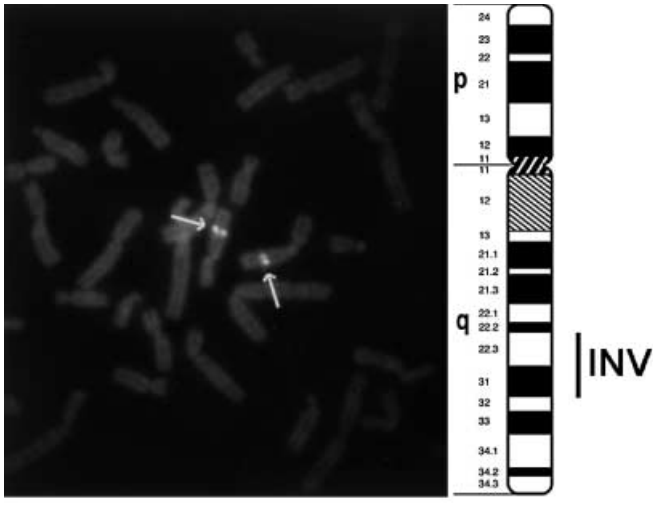

Fig. 5 FISH showing localization of hybridization signal to both chromosomes 9 in metaphase spreads. *Right* Ideogram of human chromosome 9 showing the mapped position of the *INV* gene (*vertical bar*)

of cardiac malformations, 14 had ciliary dyskinesia of the respiratory tracts, and seven had extra-hepatic biliary atresia with polysplenia. This later group was phenotypically similar to the *inv* transgenic mouse.

Mutation screening was carried out by SSCP and sequencing. We found two polymorphisms in the coding sequence of the *INV* gene and located in exon 14: a 2402 (G→A) transition changing a Gly at position 801 to a Glu (GGA to GAA), and a 2412 (C→T) transition with no amino acid change (TCC to TCT, Ser). These variations were considered as polymorphisms because they either changed a mouse-to-human non-conserved amino acid or did not change the translated amino acid. Moreover, they were present on control DNAs. One mutation was present in a Turkish family living in Germany (Fig. 6A). Five children were born to consanguineous healthy parents. A girl presented with situs inversus, ventricular septal defect, and L-transposition of the great arteries. Her younger brother had situs inversus, atrial and ventricular septal defects, and partial anomalous pulmonary venous return. Another child died from unknown causes. The mutation disrupts the consensus donor site of exon 13 (2069+2, T→C; Fig. 6B). This mutation was confirmed by digesting the PCR product with *BspMI*, a restriction site specific to the defect. Splicing was tested on lymphocyte mRNA from each family member from whom lymphocyte mRNA was available. In addition to the expected band, two additional bands were observed in the two unaffected children (II2, II4) and their affected brother (II5; Fig. 6C). Unfortunately, no RNA was available from the parents or one affected child (II3), but it is expected that they had the same splicing pattern. These two aberrant splicing bands were cloned and sequenced. They result from the skipping of exon 13 and the skipping of exon 13 and part of exon 14 with a spurious AG acceptor site (Fig. 6D). In both cases, the aberrant splicing leads to a frameshift and rapid occurrence of a stop codon. These frameshifts truncate the first IQ domain and remove both NLS-BP motifs and the second IQ domain. Exon 12 and beginning of exon 14 together with flanking intronic sequence were checked by PCR sequencing in both directions to ensure that no other mutations could account for these aberrant splicings. Surprisingly, both affected children were heterozygous for this mutation, and the normal allele produced a normal mRNA band (Fig. 6C). No other mutation could be identified in *INV*. Moreover, both parents and the two normal children were also heterozygous for this mutation. None of the 150 control individuals tested had such a mutation. Since di- or trigenism might be involved in the lateralization defect, we screened for mutation genes that are known to be associated with the lateralization defect in humans: *ZIC3* (Gebbia et al. 1997), *NODAL* (Gebbia et al. 1997), *LEFTY1*, *LEFTY2* (Kosaki et al. 1999a), *ACVR2B* (Kosaki et al. 1999b), and *CFC1* (Bamford et al. 2000). No mutation was found in either of the two affected children.

Discussion

INV codes for a peptide with an N-terminal half that contains 16 ankyrin repeats. Ankyrin is one of the most common protein sequence motifs. The discovery of 24 copies of this sequence in the cytoskeletal protein ankyrin led to the naming of this motif as the ankyrin repeat (Rubtsov and Lopina 2000). The role of ankyrin repeats in mediating protein-protein interactions has been well documented (Sedgwick and Smerdon 1999). Nevertheless, there is a

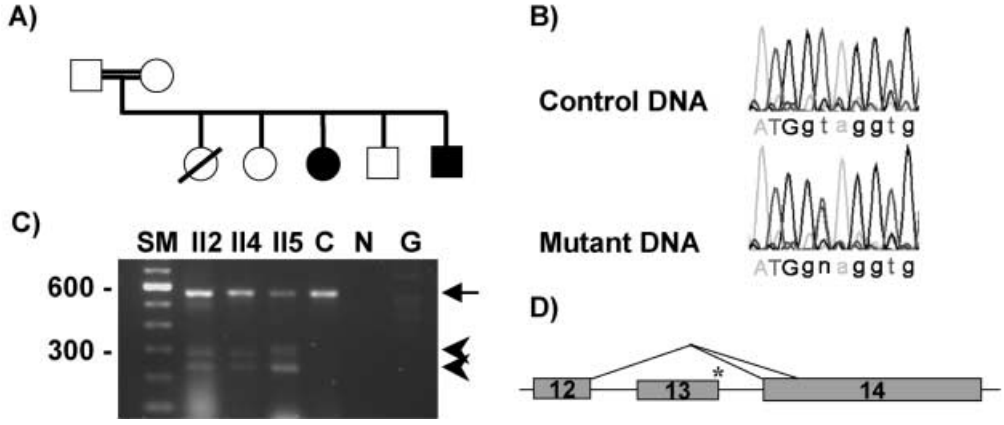

Fig. 6 **A** Pedigree of the family. Parents are first degree cousins. *Filled symbols* Children with lateralization defect and heart malformations. **B** Sequence electrophoregrams of a control DNA (*top*) and an affected child II3 (*bottom*). *Upper case* Coding nucleotides, *lower case* intronic nucleotides, *n* position at which family members were T/C heterozygous. **C** RNA extracted from transformed lymphocytes was used for RT-PCR. Primers for PCR are in exons 12 (sense) and 14 (reverse). *Left* Sizes indicated in base pairs. *SM* Size marker (a 100-bp ladder), *II2, II4, II5* pedigree positions as above, *C* control RNA, *N* RT-PCR with no RNA, *G* RT-PCR with genomic DNA. A normally spliced product (572 bp) together with additional bands were observed. The shortest bands were gel-purified, cloned, and sequenced: the 288-bp band corresponds to exon 13 skipping, the 239-bp band corresponds to skipping of exon 13 and 49 bp of exon 14 where an AG is utilized as a cryptic acceptor site. The ratio of the normal band to the additional bands varied from one amplification to the other, but the smallest bands were always present in mutant carriers and never in non-mutant carriers. **D** Scheme of the various splicings. *Star* Position of the mutation

considerable variation among ankyrin motifs. Not only is the number of repeats within any one protein highly variable (from 1 to more than 20), but also ankyrin repeats can sustain a considerable variety of amino acid substitutions and residue insertions between or within repeats. As a consequence, the length of a repeat varies from one repeat to the other, as can be seen in Fig. 2. In any case, ankyrin repeats consist of pairs of antiparallel α-helices stacked side by side and connected by intervening β-hairpin motifs. This assembled structure has been compared with a cupped hand with the β-hairpins forming the fingers and the α-helical bundle forming the palm. It is noteworthy that the ankyrin motif is highly conserved between mouse inv and human INV suggesting that the interaction with the partner protein is highly specific and that the interacting domain of the target molecule is also highly interspecies-conserved. From the various domains of INV, it can be speculated that INV is a component of a molecular complex aimed at controlling the transcription of other genes. Nevertheless, its activity is not restricted to lateralization determination, since it is expressed at low levels in a large number of adults tissues. Curiously, the IQ domains bind calmodulin, a calcium-binding peptide. Moreover, the binding of calmodulin to the distal IQ domain is critical for normal lateralization, since the absence of binding results in randomized left-right asymetry in *Xenopus* embryos (Y. Yasuhiko, F. Imai, K. Ookubo, Y. Takakuwa, K. Shikawa, T. Yokoyama, personal communication). Although inv has two NLSs, transfection assay has shown that the protein is localized in the cytoplasm (Yokoyama et al. 2001). More experiments are required to complete our understanding of INV functions and its binding partners, in particular those that interact with the ankyrin domains.

They are several lines of evidence that support the hypothesis that the splicing defect identified in this consanguineous family is causally involved in the lateralization defect. First, we have demonstrated that this variation is responsible for two aberrant splicing isoforms. The resulting truncated protein retains its binding capacity, since the ankyrin repeats are untouched, but both NLS-BP and the distal IQ motifs are lost. If this peptide is synthesized, it could still trap the interacting molecule. Second, this sequence variation has not been observed in a large series of controls that include several natives from Turkey. It is however confusing that all family members are heterozygous for the same mutation when only two have overt phenotypic anomalies. We cannot totally rule out that a minor lateralization defect has remained undisclosed after the clinical examination, electrocardiograph, and chest X-ray that all family members have undergone. None of them have reported respiratory or renal problems that could be evoked by the presence of ciliary dysfunction or renal cysts. Incomplete penetrance in the lateralization defect has previously been documented in a male carrying a nonsense mutation on his unique *ZIC3* gene copy (*ZIC3* is on chromosome X), whereas his two nephews carrying the same mutation died from severe malformations (Mégarbané et al. 2000). Penetrance might be controlled by other genetic factors; therefore, we have screened all the genes previously implicated in human lateralization defects. None of these genes had any anomaly. Other genes involved in ciliary biogenesis and function, such as *Kif3A*, *Kif3b*, *lrd*, and *polaris*, were not tested, although defects in these genes affect node monocilia vortexing in the mouse, a process essential for the proper migration of factors initiating lateralization.

So far, it can be speculated from this work and previous reports (Gebbia et al. 1997; Kosaki et al. 1999a, 1999b; Bamford et al. 2000) that autosomal recessive in-

heritance in lateralization defect is rare. In animal models, including *iv* (Hummel and Chapman 1959) and *inv* (Yokoyama et al. 1993), and in humans when lateralization defect is associated with primary ciliary dyskinesia (Kartagener syndrome; Guichard et al. 2001), lateralization defects may be inherited as an autosomal recessive trait. In contrast, the mutation screening of candidate genes in a large series of lateralization defect in humans has failed so far to find evidence of such a transmission mode (this report; Gebbia et al. 1997; Kosaki et al. 1999a, 1999b; Bamford et al. 2000). In this respect, it is surprising that we have not been able to find evidence for a mutation in the *INV* gene, even in a series of patients who have, as in the *inv* transgenic mouse, hepatic and heterotaxic anomalies. Di- or trigenism has been suggested to be the underlying inheritance mode in humans (Casey 1998) and there is some evidence from mouse (Collignon et al. 1994) and humans (Gebbia et al. 1997) to support this hypothesis. This mode of inheritance is also responsible for vertebral anomalies in *Hox* genes. For instances, compound heterozygotes (*hoxa-3*$^{-}$ /*hoxa-3*$^{+}$; *hoxd-3*$^{-}$ /*hoxd-3*$^{+}$) show a more severe mutant phenotype at higher penetrance than mice heterozygous for the *hoxd-3*$^{-}$ mutation alone (Condie and Cappechi 1994). Moreover, *hoxb5* and *hoxb6* transheterozygotes (*hoxb-5*$^{-}$ *hoxb-6*$^{+}$/*hoxb-5*$^{+}$ *hoxb6*$^{-}$) show evidence of nonallelic noncomplementation, since, for the specification of a particular region of the mammalian vertebral column, compound heterozygosity has the same consequence as homozygosity for one or the other gene (Rancourt et al. 1995). In humans, familial cases of digenism are rare. It has been reported in retinis pigmentosa (Kajiwara et al. 1994) and Waardenburg type 2 ocular albinism (Morell et al. 1997). Interestingly, in retinitis pigmentosa, evidence from family trees mimics autosomal dominant or recessive inheritance (Kajiwara et al. 1994). If we make the assumption that the lateralization defect in the family reported in this work results only from genetic factors, then at least three genetic factors ought be implicated. Since a girl is affected but not her mother, an X-linked factor in combination with an *INV* mutation cannot resolve this pedigree, because this X-linked factor would be presumably transmitted from the mother to the affected daughter, so that mother and affected daughter would have the same genotype. A second autosomal factor cannot resolve the problem in combination with the *INV* mutation, because one of the parent would have the same genetic factors as the two affected children, but be normal. Trigenism would be consistent with the pedigree: both parents carry a different predisposing factor in addition to the common *INV* mutation, and the lateralization defect results from triple heterozygosity. Alternatively, consanguinity could favor homozygosity of a mutant allele in a gene referred to as suppressor gene with no phenotypic consequence as long as a target gene has no mutation. A single mutant allele of this target gene would have no phenotypic consequence unless the mutant suppressor allele is present in two copies. This concept has previously been proposed by Beckmann (1996) and referred to as "the Réunion Island paradox" (Beckmann 1996). In this hypothesis, the *INV* gene would be the "target" gene.

In addition to environmental and genetic factors, other undisclosed factors might underpin phenotypic variability, as suggested by the mouse with the *iv* mutation in *lrd*. Mice homozygous for the *iv* mutation express a considerable variety of phenotypes ranging from total reversal of asymetry to a completely normal phenotype and including situs ambiguus (partial reversal of asymetry) (Hummel and Chapman 1959). This wide spectrum of phenotypes is obtained in a homogeneous environment and genetic background, suggesting that some natural process generates variability, independent of environmental and genetic factors. This process is thought to be randomization, because, in the absence of a coordinated molecular determination of lateralization, organ positioning would be randomized. This could explain why two out of six members of our Turkish family (and perhaps even seven members if the common mutation-carrying ancestor is included) have anomalies.

Acknowledgements We are indebted to the patients for their partipation. We thank Prof. Olivier Bernard and his collaborators at the Department of Pediatric Hepatology, Hôpital Bicètre, Le Kremlin Bicètre, France for providing us with DNA samples from patients with bilary atresia and lateralization defect. This work was supported by the Fondation de la Recherche Médicale and the Région Rhône-Alpes. Patric Schön is a recipient of a stipend from Association of European Paediatric Cardiologists (AEPC). Cécile Guichard is a student of the Ecole Pratique des Hautes Etudes, Paris; she received a stipend from SESERAC. Dr. Graham Green is gratefully thanked for editing the manuscript.

References

Alonso S, Pierpont ME, Radtke W, Martinez J, Chen SG, Grant JW, Dähnert I, et al (1995) Heterotaxia syndrome and autosomal dominant inheritance. Am J Med Genet 56:12–15

Bamford RN, Roessler E, Burdine RD, Saplakoglu U, Cruz J de la, Splitt M, Towbin J, et al (2000) Loss-of-function mutations in the EGF-CFC gene CFC1 are associated with human left-right laterality defects. Nat Genet 26:365–369

Beckmann JS (1996) The Réunion paradox and the digenic model. Am J Hum Genet 59:1400–1402

Bowers PN, Brueckner M, Yost HJ (1996) The genetics of left-right development and heterotaxia. Semin Perinatol 20:577–588

Casey B (1998) Two rights make a wrong: human left-right malformations. Hum Mol Genet 10:1565–1571

Casey B, Cuneo BF, Vitali C, Hecke H van, Barrish J, Hicks J, Ballabio A, et al (1996) Autosomal dominant transmission of familial laterality defects. Am J Med Genet 61:325–328

Chen SC, Monteleone PL (1977) Familial splenic anomaly syndrome. J Pediatr 91:160–161

Collignon J, Varlet I, Robertson EJ (1996) Relationship between asymmetric nodal expression and the direction of embryonic turning. Nature 381:155–158

Condie BG, Capecchi MR (1994) Mice with targeted disruptions in the paralogous genes hoxa-3 and hoxd-3 reveal synergistic interactions. Nature 370:304–307

Gebbia M, Ferrero GB, Pilia G, Bassi MT, Alysworth AS, Penman-Splitt M, Bird LM, et al (1997) X-linked situs abnormalities result from mutations in ZIC3. Nat Genet 17:305–308

Guichard C, Harricane MC, Lafitte JJ, Godard P, Zaegel M, Tack V, Lalau G, et al (2001) Axonemal dynein intermediate-chain gene (DNAI1) mutations result in situs inversus and primary ciliary dyskinesia (Kartagener syndrome). Am J Hum Genet 68:1030–1035

Hummel KP, Chapman DB (1959) Visceral inversion and associated anomalies in the mouse. J Hered 50:9–13

Kajiwara K, Berson EL, Dryja TP (1994) Digenic retinitis pigmentosa due to mutations at the unlinked peripherin/RDS and ROM1 loci. Science 264:1604–1608

Kosaki K, Bassi MT, Kosaki R, Lewin M, Belmont J, Schaner G, Casey B (1999a) Characterization and mutation analysis of human LEFTYA and LEFTYB homologues of murine genes implicated in left-right axis development. Am J Hum Genet 64:712–721

Kosaki R, Gebbia M, Kosaki K, Lewin M, Browers P, Towbin JA, Casey B (1999b) Left-right axis malformations associated with mutations in ACVR2B, the gene for human activin receptor type IIB. Am J Med Genet 82:70–76

Lawrence JB, Villnave CA, Singer RH (1988) Sensitive, high resolution chromatin and chromosome mapping in situ: presence and orientation of two closely integrated copies of EVB in a lymphoma cell line. Cell 52:51–61

Lindor NM, Smithson WA, Ahumada CA, Michels VV, Opitz JM (1995) Asplenia in two father-son pairs. Am J Med Genet 56: 10–11

Mathias RS, Lacro RV, Jones KL (1987) X-linked laterality sequence: situs inversus, complex cardiac defects, splenic defects. Am J Med Genet 28:111–116

Meeus A de, Sarda P, Tenconi R, Ferrière M, Bouvagnet P (1997) Blastogenesis dominant 1: a sequence with midline anomalies and heterotaxy. Am J Med Genet 68:405–408

Mégarbané A, Salem N, Stephan E, Ashoush R, Lenoir D, Delague V, Kassab R, et al (2000) X-linked transposition of the great arteries and incomplete penetrance among males with a nonsense mutation in ZIC3. Eur J Hum Genet 8:704–708

Mikkilä SP, Janas M, Karikoski R, Tarkkila T, Simola KOJ (1994) X-linked laterality sequence in a family with carrier manifestations. Am J Med Genet 49:435–438

Mochizuki T, Saijoh Y, Tsuchiya K, Shirayoshi Y, Takai S, Taya C, Yonekawa H, et al (1998) Cloning of *inv*, a gene that controls left/right asymmetry and kidney development. Nature 395: 177–181

Morell R, Spritz RA, Ho L, Pierpont J, Guo W, Friedman TB, Asher JH Jr (1997) Apparent digenic inheritance of Waardenburg syndrome type 2 (WS2) and autosomal recessive ocular albinism (AROA). Hum Mol Genet 6:659–664

Niikawa N, Kohsaka S, Mizumoto M, Hamada I, Kajii T (1983) Familial clustering of situs inversus totalis, and asplenia and polysplenia syndromes. Am J Med Genet 16:43–47

Rancourt DE, Tsuzuki T, Capecchi MR (1995) Genetic interaction between hoxb-5 and hoxb-6 is revealed by nonallelic noncomplementation. Genes Dev 9:108–122

Rubtsov AM, Lopina OD (2000) Minireview: ankyrins. FEBS Lett 482:1–5

Sedgwick SG, Smerdon SJ (1999) The ankyrin repeat: a diversity of interactions on a common structural framework. Trends Biochem Sci 24:311–316

Supp DM, Witte DP, Potter SS, Brueckner M (1997) Mutation of an axonemal dynein affects left-right asymmetry in inversus viscerum mice. Nature 389:963–966

Takahashi E, Hori T, O'Connell P, Leppert M, White R (1990) R-banding and nonisotopic in situ hybridization: precise localization of the human type II collage gene (COL2A1). Hum Genet 86:14–16

Takahashi E, Hori T, O'Connell P, Leppert M, White R (1991) Mapping of the MYC gene to band 8q24–12-q24.13 by R-banding and distal to fra(8)(q24.11), FRA8E, by fluorescence in situ hybridization. Cytogenet Cell Genet 57:109–111

Viegas-Prequignot E, Dutrillaux B (1978) Une méthode simple pour obtenir des prophases et des prométaphases. Ann Génét (Paris) 21:122–125

Yokoyama T, Copeland NG, Jenkins NA, Montgomery CA, Elder FFB, Overbeek PA (1993) Reversal of left-right asymmetry: a situs inversus mutation. Science 260:679–682

Yokoyama T, Shirayoshi Y, Murakami T, Nakatsuji N (2001) Expression of the inv gene during development and intracellular localization of the inv protein. In: Clark EB, Nakazawa M, Takao A (eds) Etiology and morphogenesis of congenital heart disease. Futura, New York, pp 15–18